Transitions to nematic states in homogeneous suspensions of high aspect ratio magnetic rods

A. Gopinath and L. Mahadevan
Division of Engineering and Applied Sciences, Harvard University, Cambridge, Massachusetts 02138

R. C. Armstrong
Department of Chemical Engineering, Massachusetts Institute of Technology, Cambridge, Massachusetts 02139

(Received 5 September 2005; accepted 31 December 2005; published online 7 February 2006)

Isotropic-nematic and nematic-nematic transitions from a homogeneous suspension of high aspect ratio magnetic rods are studied for both Maier-Saupe and Onsager excluded volume potentials. Asymptotic analysis in the vicinity of critical points yields insight into the stability and type of polarized nematic states emanating from nonpolarized equilibrium states. This, in conjunction with recently published global numerical results, yields a unified picture of the bifurcation diagram and provides a convenient base state to study effects of external orienting fields. © *2006 American Institute of Physics*. [DOI: 10.1063/1.2167811]

Recently, a model for dispersions of acicular magnetic particles was developed[1,2] using ideas grounded in classical models for liquid-crystalline polymers.[3] Effects of Brownian motion, anisotropic hydrodynamic drag, a steric force chosen to be of the Maier-Saupe form and a mean-field magnetic potential were included. Equations for order parameters obtained via closure approximations as well as more detailed diffusion equations were solved numerically.[1]

Although considerable insight is obtained via these large-scale numerical solution schemes, inherent symmetries and degeneracies imply that results obtained have to be interpreted carefully—see, for example, Ref. 4. In such cases, theoretical results, even if limited, can be used to guide efficient numerical calculations. Indeed, such an approach has been used with excellent results by Forest and co-workers (see Refs. 5 and 6 and references therein) for the case of nonmagnetic nematic rods in shear or extensional flows. In this spirit, it is pertinent to seek a theory for a simple but nontrivial base problem intricately related to the complete problem at hand. The aim of this Brief Communication is precisely this. We study transitions to nematic states from a homogeneous base state of a suspension of very slender magnetic particles in the absence of any external orienting fields. A combination of local stability analysis and available global numerical results yields a picture of possible solutions and the symmetries they satisfy. Both Maier-Saupe and Onsager excluded volume interaction potentials are considered. Results for the Maier-Saupe case are in excellent agreement with available numerical solutions of the equations and complement recent investigations on the classical Doi model.[4]

The particles comprising the homogeneous dispersion are modelled as two point masses connected by a rigid, massless rod of length L and diameter d. These rods possess intrinsic magnetic dipoles with the magnetic moment being along the axis.[1,2] The orientation of the rod is specified by the unit vector $\mathbf{u}$ along the axis from one specified bead to its complement. In the mean-field approximation it suffices to consider one test particle in a sea of others, thereby enabling use of the one-particle orientation distribution function $f(\mathbf{u},t)$ to describe the suspension. For the case of constant rotary diffusivity[7] one can write the scaled equation,

$$\frac{\partial f}{\partial t} = \mathfrak{R}_{\mathbf{u}} \cdot [\mathfrak{R}_{\mathbf{u}} f + f \mathfrak{R}_{\mathbf{u}} (V_{EV} + V_M)]. \tag{1}$$

Here $\mathfrak{R}_{\mathbf{u}}(.)$ is the rotation operator and the potentials are measured in units of k_bT. Let us define the average of a quantity, $\mathbf{X}(\mathbf{u})$, as $\langle \mathbf{X}(\mathbf{u}) \rangle \equiv \int \mathbf{X}(\mathbf{u}) f(\mathbf{u}) d\mathbf{u}$. The excluded volume intermolecular potential for the Maier-Saupe (MS) or Onsager (O) potential can then be written

$$V_{EV}(\mathbf{u}) = \int \beta_{\mathrm{MS}/O}(\mathbf{u},\mathbf{u}') f(\mathbf{u}',t) d\mathbf{u}', \tag{2}$$

where $\beta_{\mathrm{MS}}(\mathbf{u},\mathbf{u}') = -\Pi_{\mathrm{MS}}(\mathbf{u}\cdot\mathbf{u}')^2$, Π_{MS} being a phenomenological constant proportional to the concentration of rods N, and $\beta_O(\mathbf{u},\mathbf{u}') = 2NL^2 d|\mathbf{u}\times\mathbf{u}'|$. The total potential due to the mean magnetic field, V_M, can then be written

$$V_M = -(3/2)\mathcal{B}' \langle \mathbf{uu} \rangle : \mathbf{uu} - \mathcal{A}' \mathbf{u} \cdot \langle \mathbf{u} \rangle + \mathcal{A}_o + \mathcal{B}_o. \tag{3}$$

The first term reflects a net magnetic interaction potential due to average order,[1,2] the second term is the mean-field approximation to the dipole-dipole interaction between particles, and $\mathcal{A}_o$ and $\mathcal{B}_o$ are constants independent of $\mathbf{u}$.

Equations (1)–(3) exhibit rotational symmetry and imply the absence of preferred orienting directions. Clearly, the isotropic state (I) has no orientation. Nematic states (N) that are also solutions do possess intrinsic direction (characterized by the *director*), but this can vary at random. A convenient way to incorporate these symmetries is to write $\mathbf{u} = (\sin\theta \sin\phi)\mathbf{e}_x + (\sin\theta\cos\phi)\mathbf{e}_y + (\cos\theta)\mathbf{e}_z$ and express $f(\mathbf{u},t)$ in terms of the spherical harmonic functions $Y_l^m(\mathbf{u}) = Y_l^m(\theta,\phi)$, with $\mathbf{e}_z$ being the axis from which θ is measured. The constraint that f be real yields

$$f(\mathbf{u},t)=\sum_{l=0}^{\infty}\sum_{m=-l}^{+l} b_l^m(t)Y_l^m(\mathbf{u}), \tag{4}$$

where $b_l^{-m}(t)=(-1)^m\overline{b_l^m(t)}\,\forall\,(m\geqslant 0)$ with the overbar denoting complex conjugation and $b_0^0=(4\pi)^{-1/2}\,\forall\,t$ due to the normalization condition. Nematic states with fore-aft symmetry satisfy $f(\mathbf{u})=f(-\mathbf{u})$, and for these l is restricted to the set of even integers.

The macroscopic state of the suspension can be quantified by three variables: the structure tensor, $\mathbf{S}\equiv\langle\mathbf{uu}\rangle-\boldsymbol{\delta}/3$, the concomitant scalar structure factor $S_e\equiv[9(\mathbf{S}\cdot\mathbf{S}\cdot\mathbf{S})/2]^{1/3}$, and the mean polarity $\mathbf{J}\equiv\langle\mathbf{u}\rangle$. For later use, we specify two inner products: $\langle Y_l^m|f\rangle\equiv\int\overline{Y_l^m(\mathbf{u})}f(\mathbf{u},t)d\mathbf{u}$, and $\langle l_1,m_1|l_2,m_2|l_3,m_3\rangle\equiv\int\overline{Y_{l_1}^{m_1}(\mathbf{u})}Y_{l_2}^{m_2}(\mathbf{u})Y_{l_3}^{m_3}(\mathbf{u})d\mathbf{u}$, and functions $d_{2n}=[\pi(4n+1)(2n-3)!!(2n-1)!!][2^{(2n+2)}n!(n+1)!]^{-1}$ and $c_o(l')=[(l'-1)(l'-3)!!^2][(l'+2)(l'!!)^2]^{-1}$. Using these and expansion (4), one can rewrite (2) as

$$V_{\mathrm{MS}}=-\frac{3}{2}U\left(\frac{8\pi}{15}\right)\sum_{l'=0}^{\infty}\sum_{m'=-l'}^{l'}\delta_{l',2}Y_{l'}^{m'}(\mathbf{u})b_{l'}^{m'}, \tag{5}$$

and

$$V_O=-4\pi U\sum_{l'=1}^{\infty}\sum_{m'=-2l'}^{+2l'}\frac{d_{2l'}}{(4l'+1)}Y_{2l'}^{m'}(\mathbf{u})b_{2l'}^{m'} \tag{6}$$

with $U=2NL^2d$. In writing (5) and (6) we have ignored constants linear in U and independent of $\mathbf{u}$. The expressions are the same as those for nonmagnetizable rods because the excluded volume potential is just dependent on *geometrical* symmetries. Parameters $\mathcal{A}'$ and $\mathcal{B}'$ in (3) are proportional to the number density of rods, and can be rewritten as $\mathcal{A}'\equiv\mathcal{A}U$ and $\mathcal{B}'\equiv\mathcal{B}U$. Henceforth U, $\mathcal{A}$, and $\mathcal{B}$ are treated as three independent parameters. Combining (1) and (3)–(6) yields the following evolution equation for mode b_l^m,

$$\frac{db_l^m}{dt}=-l(l+1)b_l^m-\sum_{p=0}^{\infty}\sum_{q=-p}^{+p}(\sigma_{EV}+\sigma_M), \tag{7}$$

where

$$\sigma_M=4\pi U\sum_{l'=0}^{\infty}\sum_{m'=-l'}^{+l'}b_p^q b_{l'}^{m'}\left(\frac{\mathcal{B}\delta_{l',2}}{5}+\frac{\mathcal{A}\delta_{l',1}}{3}\right)\Psi \tag{8}$$

and σ_{EV} depends on the nature of the excluded volume potential,

$$\sigma_{\mathrm{MS}}=\frac{4\pi U}{5}\sum_{l'=0}^{\infty}\sum_{m'=-l'}^{+l'}b_p^q b_{l'}^{m'}\delta_{l',2}\Psi, \tag{9}$$

or

$$\sigma_O=4\pi U\sum_{l'=0}^{\infty}\sum_{m'=-2l'}^{+2l'}\frac{d_{2l'}}{4l'+1}b_p^q b_{l'}^{m'}\Psi, \tag{10}$$

with

$$\begin{aligned}\Psi(l,m,p,q,l',m')=&-mm'\langle l,m|p,q|l',m'\rangle-\frac{1}{2}\left(\frac{[l(l+1)-m(m+1)]}{[l'(l'+1)-m'(m'+1)]^{-1}}\right)^{1/2}\langle l,m+1|p,q|l',m'+1\rangle\\&-\frac{1}{2}\left(\frac{[l(l+1)-m(m-1)]}{[l'(l'+1)-m'(m'-1)]^{-1}}\right)^{1/2}\langle l,m-1|p,q|l',m'-1\rangle.\end{aligned} \tag{11}$$

Examination of (7)–(11) shows that it is possible to have solutions that comprise only modes with even index l—this implies that nematic branches corresponding to $\mathcal{A}=0$, $\mathcal{B}\geqslant 0$ and thus $J=0$ form a subset of possible stationary solutions to (7). Note that $(S=0,J\neq 0)$ states are un-physical due to the way even and odd l modes are coupled.

A linear stability analysis of (7) about the isotropic state, $f_o(\mathbf{u})=(4\pi)^{-1}$ is readily performed using $b_l^m=(b_l^m)_o+\epsilon b_l'^m+O(\epsilon^2)$, ($\epsilon\ll 1$ being a suitable amplitude) and retaining terms through $O(\epsilon)$. The growth rates λ_l^m corresponding to the disturbance $Y_l^m(\mathbf{u})$ can be obtained from the linearized equations.

For the Maier-Saupe potential, the growth rates for odd and even l, respectively, are $(\lambda_l^m)_{\mathrm{MS}}=-l(l+1)(1-\delta_{l,1}\mathcal{A}U/3)$ and $(\lambda_l^m)_{\mathrm{MS}}=-l(l+1)(1-U(1+\mathcal{B})\delta_{l,2}/5)$, indicating that the $S=0$ isotropic branch has two critical points. At the first critical point, $(1+\mathcal{B})U_c^a=5$, a *fivefold* degenerate eigenvalue set is seen with the destabilizing eigenvectors being linear combinations of Y_2^m with $m=(-2,-1,0,1,2)$. At the second critical point, $U_c^b=3\mathcal{A}^{-1}$, the critical eigenvalues that change sign are *threefold* degenerate and correspond to the eigenvectors Y_1^m with $m=(-1,0,1)$. In Fig. 1 we plot these analytical predictions and compare them to numerically obtained solutions[1] for the case $\mathcal{B}=1$. We note that for fixed and finite $\mathcal{B}$, as $\mathcal{A}\to\infty$, $U_c^b\to 0$. As $\mathcal{A}$ decreases from very large values, $U_c^b<U_c^a$ initially and then, beyond a critical value of $\mathcal{A}$, we get $U_c^b>U_c^a$. For $\mathcal{B}=1$, the two critical points coincide for $\mathcal{A}=1.2$. Detailed numerical calculations show that for $U_c^b<U_c^a$, the bifurcating nematic branch is prolate, otherwise it is an oblate branch.

For the Onsager potential, the eigenvalues for odd and even l are $(\lambda_l^m)_O=-l(l+1)(1-\mathcal{A}U\delta_{l,1}/3)$ and $(\lambda_l^m)_O=-l(l$

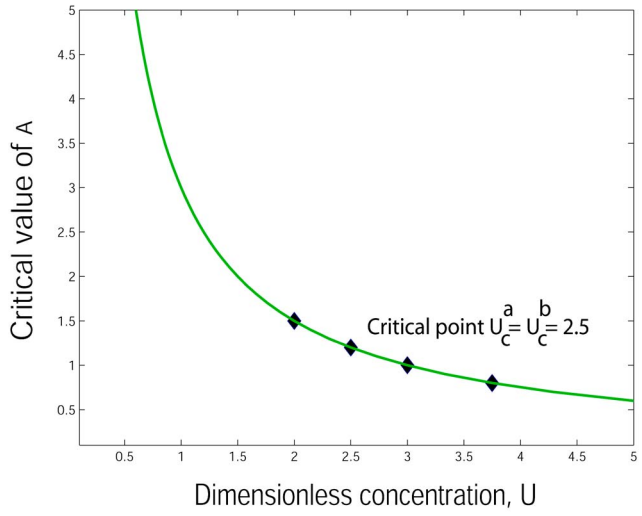

FIG. 1. A plot of $\mathcal{A}(U)$ at which the instability to $Y_1^m, m=-1,0,1$ modes arises on the isotropic $J=S=0$ branch for the Maier-Saupe potential. The diamonds are renormalized computed results obtained from a numerical solution for $\mathcal{B}=1$ from Bhandar (Ref. 1).

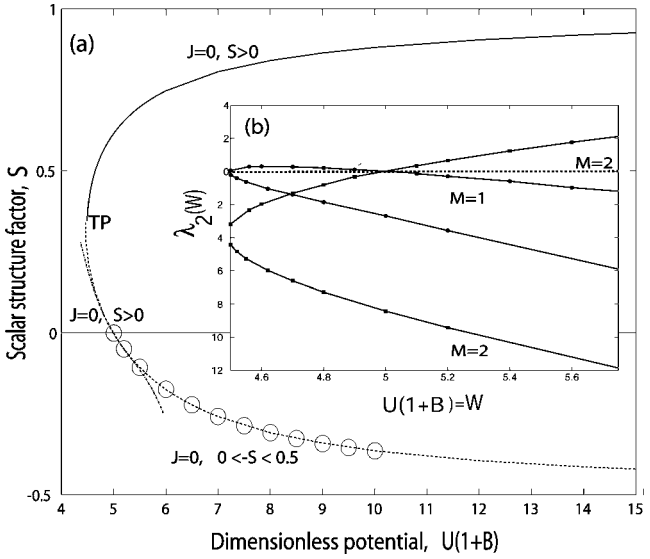

FIG. 2. (a) The equilibrium bifurcation diagram of the base nematic states with $J=0$ for $\mathcal{A}=0$. The prolate branch arising from U_c^a is unstable to structure factor fluctuations but regains stability beyond the turning point at $W=U(1+\mathcal{B})\approx 4.49$. The dash-dot line is the curve corresponding to the asymptotic expansion. Inset: (b) Eigenvalues corresponding to the destabilizing eigenvectors Y_2^m at U_c^a when $\mathcal{A}=0$. M denotes multiplicity.

$+1)[1-U(1+\mathcal{B})\delta_{k,1}/5+U\pi c_o(l)/2]$. Thus for odd l, as for the Maier-Saupe potential, there is one critical point on the $S=0$ line, viz U_c^b. The destabilizing eigenvectors are, as before, the three independent components of $Y_1^m(\mathbf{u})$. Let us denote the critical points for even l by $U_c^a(l)$ such that the critical eigenvectors at each point are the $2l+1$ independent components of $Y_l^m(\mathbf{u})$. The first critical point occurs at $U_c^a(2)=[\pi c_o(2)/2+\mathcal{B}/5]^{-1}$ and corresponds to the eigenvector set $Y_2^m(\mathbf{u})$. Higher-order bifurcations (for $l\geqslant 4$) occur at $U_c^b(l)=2[\pi c_o(l)]^{-1}$.

We now turn to characterizing $J>0$ branches bifurcating from the nontrivial $(J=0, S\neq 0)$ nematic states when the intermolecular potential is of Maier-Saupe type. To do that we need to delve a bit more into the nature of the $S\neq 0$, $J=0$ branches.

As mentioned earlier, Eqs. (1), (3), and (7)–(9) with $\mathcal{A}=0$ exhibit rotational symmetry and so we consider a base nematic state of the form (3) with director $\mathbf{n}=\mathbf{e}_z$ such that $\cos\theta=(\mathbf{u}\cdot\mathbf{n})$ and coefficients $(b_l^m)_o$ real and nonzero only if *both* l and m are even. The potential U and the parameter $\mathcal{B}$ can be combined into one dimensionless factor, $W=U(1+\mathcal{B})$. Then the steady, uniaxial base solutions are of the form $f_o(\theta)=\exp(3WS\cos 2\theta/4)/P$, P being a normalizing constant. Substituting this in (1) yields

$$\frac{2S+1}{3}=\left[\int_0^1 \exp\left(\frac{3}{2}WSt^2\right)t^2dt\right]\Bigg/\left[\int_0^1 \exp\left(\frac{3}{2}WSt^2\right)dt\right]$$

plotted in Fig. 2(a). The solid lines are linearly stable branches. The oblate phase where the rods are oriented randomly in the $(\boldsymbol{\delta}-\mathbf{nn})$ plane, is unstable to director fluctuations but stable if these are suppressed; specifically, the open circles are solutions obtained via time integration of (1) in such a special subspace.[4] Brownian dynamics simulations of the system for the Maier-Saupe potential[8] and $\mathcal{B}_m=0$ indicate that results using time integration for short times can yield an apparently stable oblate phase, thus mimicking the effect of a pinned director. However, long time integration of the stochastic system leads to the oblate branch being destabilized by perturbations to the director. Similar considerations hold for $\mathcal{B}\geqslant 0$. A regular perturbation expansion in the small parameter, $\hat{W}\equiv W-5$ indicates that along the nematic branches, we have for $|\hat{W}/5|\ll 1$

$$S(\hat{W})\approx -\frac{7}{25}\hat{W}+\frac{119}{625}\hat{W}^2-\frac{29\,981}{17\,1875}\hat{W}^3, \tag{12}$$

also plotted in Fig. 2(a) as the dash-dot line. The structure factor for these base nematic states has the form $\mathbf{S}_o=-S(W)\mathbf{S}^{(1)}/3$, where $S_{xx}^{(1)}=S_{yy}^{(1)}=-S_{zz}^{(1)}/2$ with other terms being zero. Critical eigenvalues corresponding to the destabilizing eigenvectors Y_2^m are shown in the inset. There are five eigenvalues that are zero at U_c^a, of which three attain nonzero values along the nematic branches. The eigenvalue corresponding to Y_2^0 (the structure parameter mode) has multiplicity $M=1$. The other four correspond to director fluctuations and occur in two pairs. Since there are two independent ways to rotate a director on a sphere, we expect two neutral eigendirections (or two zero eigenvalues) along each $S\neq 0$ branch.

Are there critical points on these $J=0$ nematic branches where instability to the $l=1$ mode sets in? As a point of departure to frame our answer, we focus on the vicinity of the critical concentration $U_c^a=U_c^b$ and study bifurcations as $\mathcal{A}$ and U are varied with $\mathcal{B}$ held fixed. Impose small perturbations to the base state, $b_l'^m$, comprised only of even m modes while l can be both even and odd. The equation for the growth of mode $b_1'^0$ with $\Psi_{(1)}=\Psi(1,0,2,0,1,0)=1/\sqrt{(5\pi)}$ and $\Psi_{(2)}=\Psi(1,0,1,0,2,0)=-3/\sqrt{(5\pi)}$ is then

$$\frac{db_1'^0}{dt} = -2b_1'^0\left(1 - \frac{U\mathcal{A}}{3} + \frac{2\pi U\mathcal{A}}{3}(b_2^0)_o\Psi_{(1)}\right) - \frac{4\pi U}{5}(1+\mathcal{B})\sum_{p=0}^{\infty}\sum_{q=-p}^{+p}\sum_{m'=-2}^{2} b_p'^q(b_2^{m'})_o \times \Psi(1,0,p,q,2,m'). \quad (13)$$

Close to criticality, the $b_1'^0$ mode dominates. A good approximation for small S can be obtained by ignoring the $p=3$ term in (13) and setting the growth rate to zero,

$$\left[1 + \frac{2\pi}{5}(1+\mathcal{B})U(b_2^0)_o\Psi_{(2)}\right] = \frac{U\mathcal{A}^c}{3}[1 - 2\pi(b_2^0)_o\Psi_{(1)}], \quad (14)$$

valid close to the critical point $U_c^a(=U_c^b)$. Now we expand all quantities in terms of a small parameter δ [distance from the critical point along the $(J=0)$ branches] to obtain the following: (a) $U=5(1+\mathcal{B})^{-1}(1+\delta\hat{U})$, (b) $\mathcal{A}^c=3(1+\mathcal{B})(1+\delta\hat{\mathcal{A}}^c)/5$, and (c) $(b_2^0)_o=\delta(\hat{b}_2^0)_o \approx \delta U'(d/d\hat{U})_0(\hat{b}_2^0)_o=\delta k_m\hat{U}$ with the slope $k_m=-7\sqrt{5}(10\sqrt{\pi})^{-1}$. Substituting these in (14) yields at $O(\delta)$

$$\hat{\mathcal{A}}^c = [2\pi(\Psi_{(1)}+\Psi_{(2)})k_m - 1]\hat{U} = 9\hat{U}/5. \quad (15)$$

Thus, close to the critical point as we move along the prolate with $\hat{U}$ locally decreasing, $\hat{\mathcal{A}}^c$ decreases as well. As one moves along the oblate towards more higher values of U (i.e., $\hat{U}$ increases), $\hat{\mathcal{A}}^c$ increases. In short, critical points on the $(J=0, S<0)$ oblate state have $\mathcal{A}^c>1.2$ and on the $(J=0, S>0)$ prolate state satisfy $\mathcal{A}^c<1.2$.

Though asymptotic in nature, our local linear analysis accords very well with global numerical solutions (far from the critical point) obtained by Bhandar[1] for $\mathcal{B}=1$. A combination of the two yields the scenario depicted in Fig. 3. Let us recast the results in terms of the dependence of $\mathcal{A}^c$ on the scalar structure parameter. For a fixed value of $\mathcal{A}$, there are two critical points at which the $J=0$ branch becomes unstable to disturbances comprised of Y_1^0 components. One of them is always on the $(S=0, J=0)$ isotropic branch and the other is always on the $(S\neq 0, J=0)$ nematic solution. When $\mathcal{A}<1.2$, the $J>0$ branches bifurcate at one point in the segment $(S=0, U>5/2)$ and at one point in the prolate branch $(J=0,\ S>0)$. Even though the $J=0$ nematic prolate has a turning point at $U\approx 2.245$, the salient qualitative results of the local analysis holds even far from the critical point.[9]

Consider now the effects of an imposed external magnetic field $\mathbf{H}$ modeled by adding a term proportional to $\mathbf{u}\cdot\mathbf{H}$ to the potential to (1) and (3). Such a field breaks the rotational degeneracy of the system by introducing a natural orienting direction. We anticipate that for fixed values of U, $\mathcal{A}$, and $\mathcal{B}$, the degree of order S, as well as the extent of average polarization J, change continuously with H. The transition from an isotropic to nematic state is replaced by a transition from a weakly aligned (paranematic) state to a strongly aligned state. Our results provide a mathematically convenient and physically relevant starting point to investigate these scenarios.

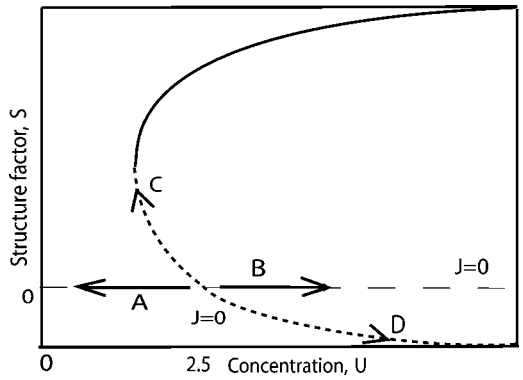

FIG. 3. Schematic sketch of the bifurcation scenario obtained by combining local analysis and global numerical results for $\mathcal{B}=1$. Region (A) corresponds to $0<U<U_c^a$, $S_e=J=0$, and $\infty<\mathcal{A}^c<1.2$. As U increases, the critical value of $\mathcal{A}$ decreases, reaching 1.2 at $U=U_c^a=5(1+\mathcal{B})^{-1}$. Region (B) corresponds to $U_c^a<U<\infty$, $S=J=0$, and $1.2<\mathcal{A}^c<0$. In region (C) $(J>0, S>0)$ nematic branches bifurcate from the $(J=0, S>0)$ prolate curve. In this region, as one moves to $S\to 1$, $\mathcal{A}^c$ decreases from 1.2 to 0. Finally, in region (D) along the oblate branch with $(J=0, S<0)$, we find $\mathcal{A}^c$ increasing from 1.2 as S decreases from 0 to $-1/2$.

A.G. thanks Dr. A. S. Bhandar for providing the numerical data used in Fig. 1 and Professor Forest for pointers to related work on liquid crystal polymer flow problems.

[1] A. S. Bhandar, "A constitutive theory for magnetic dispersions," Ph.D. thesis, The University of Alabama, 2002.
[2] A. S. Bhandar and J. M. Weist, "Mesoscale constitutive modeling of magnetic dispersions," J. Colloid Interface Sci. **257**, 371 (2003).
[3] R. G. Larson and H. C. Öttinger, "Orientation distribution function for rod-like polymers," Macromolecules **24**, 6270 (1991).
[4] A. Gopinath, R. C. Armstrong, and R. A. Brown, "Observations on the eigenspectrum of the linearized Doi equation and application to numerical simulations of liquid crystal suspensions," J. Chem. Phys. **121**, 6093 (2004).
[5] M. G. Forest, R. Zhou, and Q. Wang, "Scaling behavior of kinetic orientational distributions for dilute nematic polymers in weak shear," J. Non-Newtonian Fluid Mech. **116**, 183 (2004).
[6] M. G. Forest, Q. Wang, and R. Zhou, "The flow-phase diagram of Doi-Hess theory for sheared nematic polymers II: finite shear rates," Rheol. Acta **44**, 80 (2004).
[7] The assumption of constant diffusivity is reasonable as we are concerned only with equilibrium nematic states.
[8] C. I. Siettos, M. D. Graham, and I. G. Kevrekidis, "Coarse Brownian dynamics for nematic liquid crystals: Bifurcation, projective integration, and control via stochastic simulation," J. Chem. Phys. **118**, 10149 (2003).
[9] Bhandar's results for the prolate branch $(S\approx +0.14)$ indicate that the slope $\partial_{\hat{U}}\hat{\mathcal{A}}^c$ is around 2.08 while the results for the oblate branch $(S\approx -0.17)$ yield a value of around 1.8; both estimates are in excellent agreement with the predicted value of 9/5 in the vicinity of $S=0$.